Self-Powered Water Splitting Using Flowing Kinetic Energy

Wei Tang, Yu Han, Chang Bao Han, Cai Zhen Gao, Xia Cao, and Zhong Lin Wang**

Water splitting is utilized as a regenerative life supporting system and is part of the energy conversion process in nature. Its manipulation is often accomplished through the application of electrical potential by an external power supply.[1,2] In order to develop a cost-effective and environment friendly technology, many researchers have focused on this field.[3–7] Photocatalytic splitting of water into H_2 and O_2 using a catalyst and the solar energy is one of the ideal approaches.[2,8] Besides, biological hydrogen production processes are also found to be environment friendly and less energy intensive.[5] Among these technologies, the energy source for water splitting includes solar, chemical, and thermal energy; whereas, the mechanical energy is rarely involved,[9] which is, however, of major interest, due to its universal availability.[10–12]

Recently, the invention of triboelectric nanogenerator (TENG) has provided an effective approach to convert ambient mechanical energy into electricity.[12–23] The working principle of the TENG is based on the combination of contact electrification and electrostatic induction. Contact-induced charge transfer between two tribomaterials with opposite polarity results in a potential difference when the two materials are separated. This potential difference will drive the electrons/ions in the external circuit to flow, which could be used for water splitting.

Here in this work, we firstly develop a water splitting system that is fabricated by coupling a TENG and a water splitting unit. When the TNEG's spinning speed is 600 rpm, the hydrogen producing rate in 30% (w.t.) potassium hydroxide (KOH) solution reaches 6.25×10^{-3} mL min^{-1}. Particularly, when the KOH solution is replaced by pure water, the system is demonstrated to be even four times more effective for hydrogen generation than that driven by an electrochemical workstation at 10 V. Furthermore, the normal tap water flowing is successful to drive TENG for effectively splitting power, which shows the first fully self-powered water splitting system.

The system is composed of a TENG and a water splitting unit. The TENG has a multilayered structure, which consists of mainly two parts: a rotator and a stator, as sketched in **Figure 1**a. The whole fabrication is mainly based on the printing circuit technology,[24–27] making it of low cost and scalable production. As exhibited in Figure 1a, the rotator is a collection of radially arrayed sectors with each sector unit having a central angle of 1°. The stator comprises of three components: a layer of Kapton as an electrification material, a layer of electrodes, and an underlying epoxy glass cloth laminate sheet (FR4) as the substrate. The electrode layer is composed of two complementary-patterned electrode networks that are disconnected by fine trenches in between (Figure 1a). Due to the fabrication limit of the printing circuit technology, the pattern of each network is partly different from that of the rotator. It is formed by a radial array of sectors, with a length about 60 mm, the angle of 1°, and mutually connected at one end. Since both the rotator and the stator have 2D planar structures, the TENG takes the advantage of a small volume. The working principle of this kind of TENG was reported previously.[16,25,28] The output performance under 600 rpm is plotted in Figure 1b–e. As we can see, the short-circuit current (I_{sc}) has a continuous AC output at an average amplitude of 1 mA (Figure 1b). For the open-circuit voltage (V_{oc}), it oscillates at the same frequency as that of I_{sc} with a peak value around 240 V (Figure 1c). According to the previous work,[16,25] the continuous AC output from the rotating TENG could be tuned by using the conventional transformer, which is effective to boost the output current at the expense of the output voltage, as shown in Figure 1d, e. Therefore, the transformed current was enhanced up to 11 mA, while the voltage was reduced to about 17 V, which means the transformed efficiency is about 77.9%.

Water Splitting Experiments: The above TENG was subsequently connected with the water splitting unit. **Figure 2**a shows the schematic diagram. The TENG's output was initially transformed and rectified. As for the water splitting unit, Pt was selected as the two electrodes. 30% (w.t.) KOH solution was utilized as the electrolytes. According to the electrolysis effect, the water splitting mechanism can be explained by the following equations:

$$4OH^- \rightarrow 2H_2O + O_2 + 4e^- \text{(anode)} \quad (1)$$

$$4H^+ + 4e^- \rightarrow 2H_2 \text{(cathode)} \quad (2)$$

Therefore, O_2 and H_2 are produced at the anode and the cathode, respectively. In order to collect the H_2, the cathode was inserted into a tube, whose top end was sealed by epoxy. It can

Dr. W. Tang, Dr. C. B. Han, Prof. X. Cao, Prof. Z. L. Wang
Beijing Institute of Nanoenergy and Nanosystems
Chinese Academy of Sciences
Beijing 100083, China
E-mail: caoxia@binn.cas.cn
Y. Han, C. Z. Gao
School of Chemistry and Environment
Beijing University of Aeronautics and Astronautics
Beijing 100083, China
Prof. X. Cao
School of Biochemical and Pharmaceutical Sciences
Capital Medical University
Beijing 100069, China
Prof. Z. L. Wang
School of Material Science and Engineering
Georgia Institute of Technology
Atlanta, Georgia 30332–0245, USA
E-mail: zlwang@gatech.edu

DOI: 10.1002/adma.201404071

ADVANCED MATERIALS
www.advmat.de

www.MaterialsViews.com

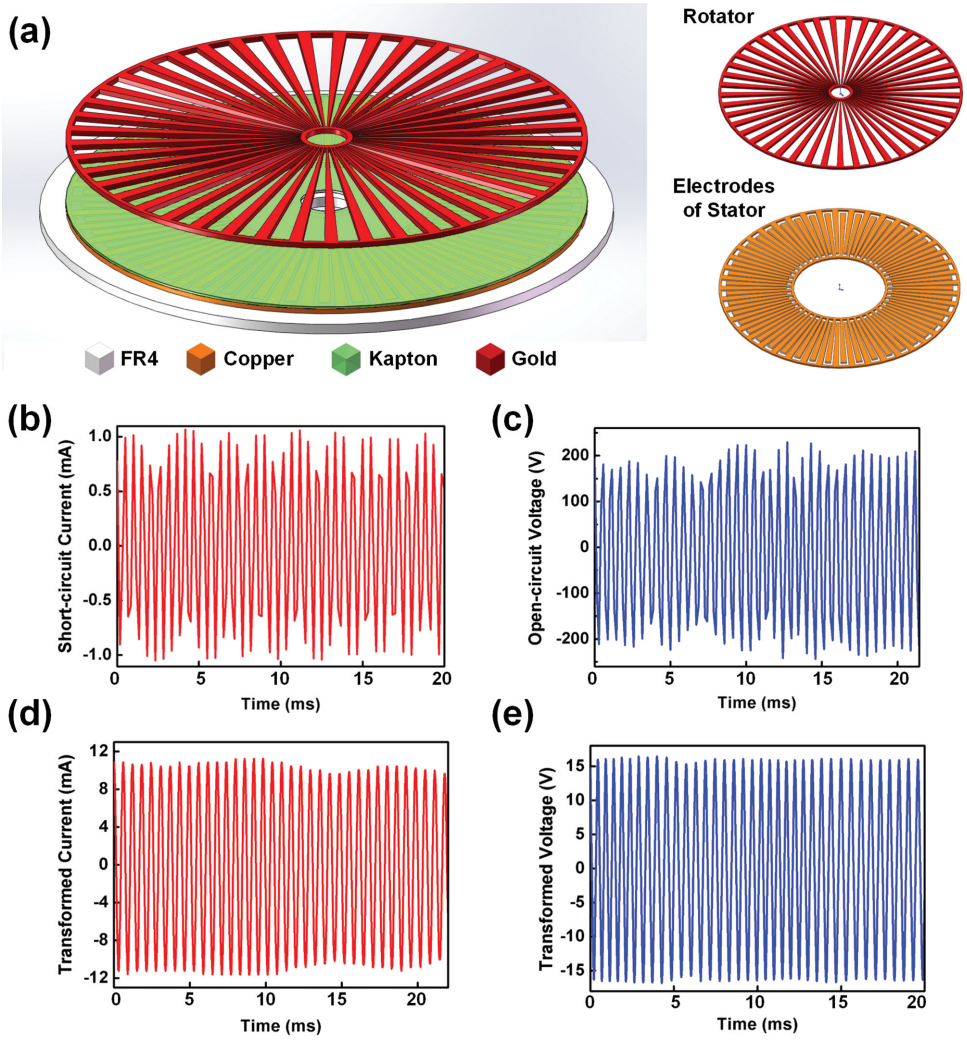

Figure 1. Structural design and characterizations of the disk TENG. a) Schematic illustrations of the disk TENG. b) The short-circuit current and c) the open-circuit voltage of the as-fabricated disk TENG. d) The short-circuit current and e) the open-circuit voltage after applying a transformer.

be seen from Figure 2a, b, that the H_2 tube was initially filled with the KOH solution and partly immersed into the beaker. When the produced H_2 was collected on the top of the tube, the solution can flow out from the collection tube due to the larger pressure of the produced H_2, resulting in the drop of water surface level in the tube. The volume and the elapsed time of the H_2 producing were recorded. Figure 2c illustrates photographs of the H_2 collection tube varying with time when the rotating speed of the assemble TENG is 600 rpm. As the volume of the generated H_2 increased with time, the solution level in the tube dropped gradually. Detailed data were plotted in Figure 2d. It apparently exhibited a linear relationship between the H_2 production volume and the splitting time, with a slope of 6.25×10^{-3} mL min^{-1}. The dynamic splitting process can be found in Movie S1 (Supporting Information).

The H_2 production rate was investigated by varying the rotating velocity of the TENG, as shown in **Figure 3**a, b. When the rotating speed was 200 rpm, the H_2 production rate was about 1.4×10^{-3} mL min^{-1}. With the speed rising to 600 rpm, the production rate increased up to 6–7 $\times 10^{-3}$ mL min^{-1}. In order to access the role of electrolytes in the splitting system, experiments were performed in different solutions, including 5% (w.t.) Na_2SO_3, 0.5 M H_2SO_4, and 30% (w.t.) KOH (TENGs' output were all transformed and rectified). It was found that, the H_2 production rates in the three electrolytes varied to some degree (Figure 3c, d). The one in the KOH solution was larger than the other two, which might be due to the higher concentration and thus the lower resistance.

Pure Water Splitting: According to the literature, electrolytes are required for water splitting to improve the conductivity in accounting for the large resistance of pure water. However, the addition of electrolytes (e.g., strong acid or alkali) might produce undesirable effects (e.g., equipment corrosion) or byproducts. Therefore, pure water was utilized in our study. Optical images are illustrated in **Figure 4**a, b. It can be seen that the electrochemical workstation with a voltage of 10 V produced one H_2 bubble after 90 s; whereas the TENG-driven system apparently produced four H_2 bubbles. As a comparison, when the output voltage of the TENG was reduced to about 10 V by a transformer, there was none

Adv. Mater. **2014**,
DOI: 10.1002/adma.201404071

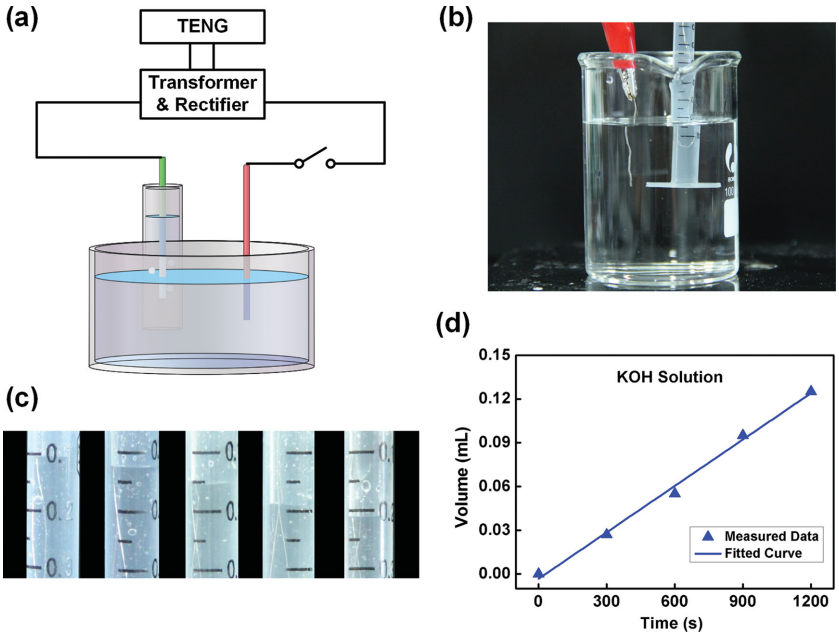

Figure 2. a) Schematic diagram of the TENG-driven water splitting system. b) The optical image of the H_2 collection tube. c) Photographs of the H_2 collection tube at the different time in KOH solution. d) H_2 production volume as a function of time.

H_2 bubble, indicating that the high voltage output of the TENG is effective for overcoming the large load resistance, namely the pure water in our work. Further experimental data confirmed this analysis. The current produced by the TENG was over four times larger than that produced by the electrochemical workstation, as well as the power-transformed TENG, in the pure water (Figure 4c).

Self-Powered Water Splitting: Our study presented above is to use a disk TENG that is driven by a motor, which is not ideal for practical applications. What we intend to do is to drive the water splitting system using the electricity harvested from the water itself, so that no external power source is needed for the water splitting. **Figure 5**a shows the experiment setup. The TENG was connected to a miniaturized water turbine, which was then driven by the flow of normal tap water at a flow rate of 3 L min^{-1}. The related outputs are presented in Figure S1 (Supporting Information). Due to the decay of the spinning speed and the driven force given by the tap water, the TENG's output current and voltage decreased to some degree. Then, the electricity generated by water flow was used to split the water. In order to present the splitting process in a visible manner, a 1000 μF capacitor was employed as a charge reservoir. The circuit diagram is shown in Figure 5b (the transformer is not used in this experiment). Electricity was first stored in the capacitor, and then used for the splitting in the KOH solution. The voltage of the capacitor was monitored and plotted in Figure 5c. As we can see, after 60 min, the capacitor was charged from 1.7 to 4.5 V.

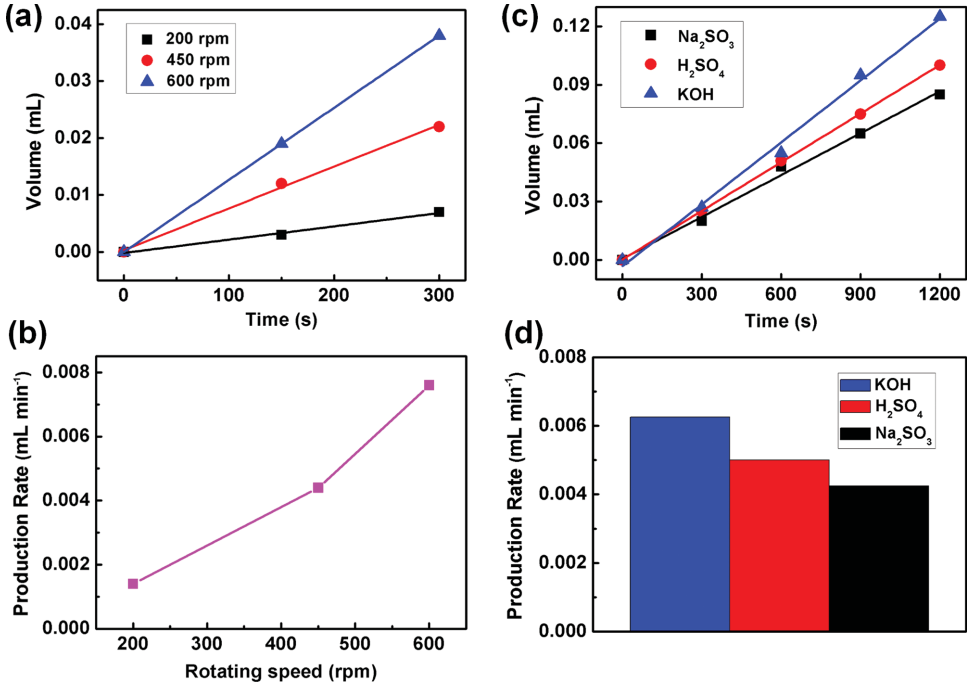

Figure 3. a) H_2 production volume as a function of the rotating speed of TENG. b) H_2 production rate as a function of the rotating speed of TENG. c,d) Dependence of the TENG-driven water splitting rate on the electrolytes.

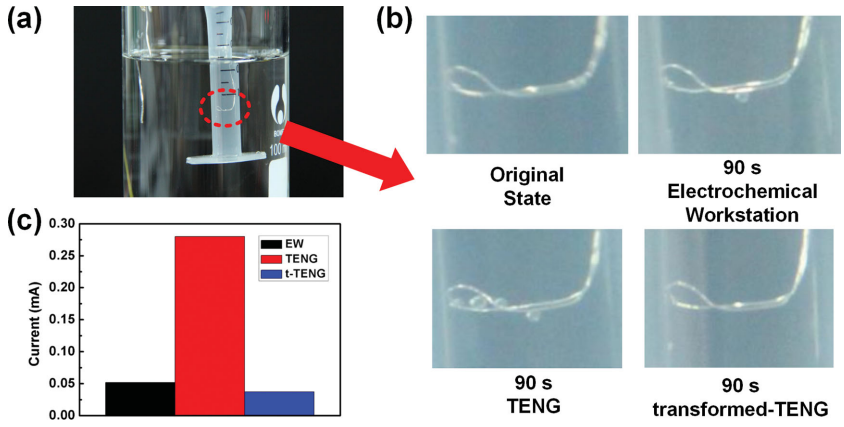

Figure 4. Pure water splitting experiment. a) Optical image of the H_2 collection tube. b) Optical images of the Pt wire, which is the enlarged view of Figure 4a. c) The current comparison in the pure water splitting system.

When being connected with the water splitting system, it discharged rapidly from 4.5 to 1.8 V (Noting that 1.8 V could be the decomposition voltage of the KOH solution in our experiments). Photographs of the splitting process are illustrated in Figure 5d. Bubbles can be apparently seen in both electrodes, which are hydrogen in the cathode, and oxygen in the anode. The volume of generated H_2 during once discharging is found to be 0.3×10^{-3} mL, which means the amount of transferred charges is about 2.57 mC and the consumed electrolytic energy is about 3.8 mJ. The amount of charges is consistent with that released by the capacitor, and the corresponding energy conversion efficiency is about 43.8%. The self-powered water splitting can be found in Movie S2 (Supporting Information).

In summary, we present here the first self-powered water splitting system by integrating a TENG and a water splitting unit. When the assembled TENG's rotating speed is 600 rpm, the system produces hydrogen with a rate of 6.25×10^{-3} mL min^{-1} in the 30%

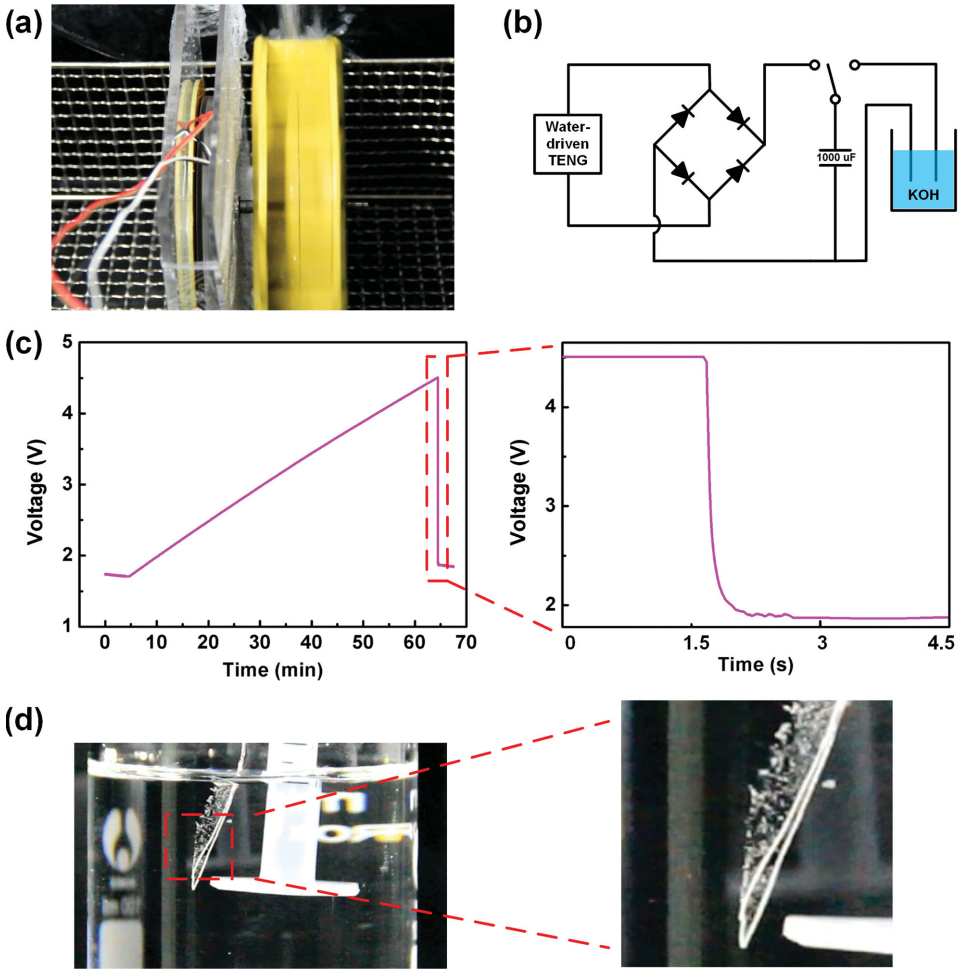

Figure 5. Self-powered water splitting. a) The TENG is assembled with a miniature water turbine. b) The circuit diagram of the self-powered water splitting system. c) The storage capacitor's working curve. d) Photographs of the self-powered splitting process, where the produced O_2 and H_2 bubbles are bursting out. This experiment proves the feasibility of fully self-powered water splitting process.

Adv. Mater. **2014**,
DOI: 10.1002/adma.201404071

(w.t.) KOH solution. When the electrolyte is replaced by pure water, the water splitting system is even 4–5 times faster than that driven by an electrochemical workstation simply because of the high voltage output of the TENG. Furthermore, the TENG can be driven by the flow of normal tap water, demonstrating the fully self-powered water splitting system. Therefore, the TENG-driven water splitting is an effective approach for in situ hydrogen generation either for energy storage or chemical reactions without an external power source. It will surely initiate a research direction in this field of triboelectrolysis and possibly impose impact on energy science.

Acknowledgements

W.T. and Y.H. have contributed equally to this work. The authors thank the support from the "Thousands Talents" program for pioneer researcher and their innovation team, China, the National Natural Science Foundation of China, the Program for New Century Excellent Talents in University (NWET-12–0610), the science and technology research projects from education ministry (213002A), National "Twelfth Five-Year" Plan for Science & Technology Support (No. 2011BAZ01B06), the Beijing Natural Science Foundation of China (Grant No. 4141002), and the China Postdoctoral Science Foundation (Grant No. 2014M550031).

Received: September 4, 2014
Revised: October 2, 2014
Published online:

[1] E. Rasten, G. Hagen, R. Tunold, *Electrochim. Acta* **2003**, *48*, 3945.
[2] D. Stojića, M. Marčetaa, S. Soviljb, Š. Miljanićc, *J. Power Sources* **2003**, *118*, 315.
[3] O. Khaselev, J. A. Turner, *Science* **1998**, *280*, 425.
[4] X. Wang, K. Maeda, A. Thomas, K. Takanabe, G. Xin, J. Carlsson, K. Domen, M. Antonietti, *Nat. Mater.* **2008**, *8*, 76.
[5] D. Das, T. Veziroglu, *Int. J. Hydrogen Energy* **2001**, *26*, 13.
[6] U. Shahed, A. Mofareh, B. William, *Science* **2002**, *297*, 2243.
[7] C. Linkous, H. Anderson, R. Kopitzke, G. Nelson, *Int. J. Hydrogen Energy* **1998**, *23*, 525.
[8] Z. Zou, J. Ye, K. Sayama, H. Arakawa, *Nature* **2001**, *414*, 625.
[9] Y. Yang, H. Zhang, Z. Lin, Y. Liu, J. Chen, Z. Lin, Y. Zhou, C. Wong, Z. L. Wang, *Energy Environ. Sci.* **2013**, *6*, 2429.
[10] Z. Wang, J. Song, *Science* **2006**, *312*, 242.
[11] S. P. Beeby, M. J. Tudor, N. M. White, *Meas. Sci. Technol.* **2006**, *17*, R175.
[12] Z. L. Wang, *ACS Nano* **2013**, *7*, 9533.
[13] F. Fan, Z. Tian, Z. L. Wang, *Nano Energy* **2012**, *1*, 328.
[14] S. Wang, L. Lin, Z. Wang, *Nano. Lett.* **2012**, *12*, 6339.
[15] L. Lin, S. Wang, Y. Xie, Q. Jing, S. Niu, Y. Hu, Z. L. Wang, *Nano. Lett.* **2013**, *13*, 2916.
[16] G. Zhu, J. Chen, T. Zhang, Q. Jing, Z. L. Wang, *Nat. Commun.* **2014**, *5*, 3426.
[17] G. Zhu, Y. Zhou, P. Bai, X. Meng, Q. Jing, J. Chen, Z. L. Wang, *Adv. Mater.* **2014**, *26*, 3788.
[18] W. Tang, C. Zhang, C. Han, Z. L. Wang, *Adv. Funct. Mater.* **2014**, *24*, 6684.
[19] C. Zhang, W. Tang, C. Han, F. Fan, Z. L. Wang, *Adv. Mater.* **2014**, *26*, 3580.
[20] X. Zhang, M. Han, R. Wang, F. Zhu, Z. Li, W. Wang, H. X. Zhang, *Nano. Lett.* **2013**, *13*, 1168.
[21] B. Meng, W. Tang, Z. Too, X. Zhang, M. Han, H. X. Zhang, *Energy Environ. Sci.* **2013**, *6*, 3235.
[22] W. Tang, B. Meng, H. X. Zhang, *Nano Energy* **2013**, *2*, 1164.
[23] Y. Yang, Y. Zhou, H. Zhang, Y. Liu, S. Lee, Z. L. Wang, *Adv. Mater.* **2013**, *25*, 6594.
[24] W. Tang, C. Han, C. Zhang, Z. L. Wang, *Nano Energy* **2014**, *9*, 121.
[25] C. Han, C. Zhang, W. Tang, X. Li, Z. L. Wang, *Nano Res.* **2014**, DOI 10.1007/s12274-014-0555-3.
[26] B. Meng, W. Tang, X. Zhang, M. Han, W. Liu, H. X. Zhang, *Nano Energy* **2013**, *2*, 1101.
[27] W. Liu, M. Han, X. Sun, B. Meng, X. Zhang, H. X. Zhang, *Nano Energy* **2014**, *9*, 401.
[28] S. Wang, Y. Xie, S. Niu, L. Lin, Z. L. Wang, *Adv. Mater.* **2014**, *26*, 2818.